

# The effect of advection on the nutrient reservoir in the North Atlantic subtropical gyre

Jaime B. Palter<sup>1</sup>, M. Susan Lozier<sup>1</sup> & Richard T. Barber<sup>2</sup>

Though critically important in sustaining the ocean's biological pump, the cycling of nutrients in the subtropical gyres is poorly understood. The supply of nutrients to the sunlit surface layer of the ocean has traditionally been attributed solely to vertical processes. However, horizontal advection may also be important in establishing the availability of nutrients. Here we show that the production and advection of North Atlantic Subtropical Mode Water introduces spatial and temporal variability in the subsurface nutrient reservoir beneath the North Atlantic subtropical gyre. As the mode water is formed, its nutrients are depleted by biological utilization. When the depleted water mass is exported to the gyre, it injects a wedge of low-nutrient water into the upper layers of the ocean. Contrary to intuition, cold winters that promote deep convective mixing and vigorous mode water formation may diminish downstream primary productivity by altering the subsurface delivery of nutrients.

Wind-driven upwelling<sup>1</sup>, diapycnal diffusion<sup>2</sup>, wintertime convection<sup>3–5</sup> and, more recently, eddy heaving<sup>6,7</sup> have all been examined for their contribution to the upward flux of nutrients in the global ocean. It is generally assumed that the variability in these vertical processes translates into variability of primary productivity. This assumption relies on the premise that an adequate reservoir of nutrients resides below the euphotic zone—this is a possibility only if the remineralization of organic matter at depth occurs much more quickly than the physical processes that move nutrients upwards. In this one-dimensional view, the downward flux of organic material from the surface ocean is balanced locally by the upward flux of nutrients from the thermocline, as discussed in ref. 8. Though conceptually appealing in its simplicity, this view not only neglects the horizontal advection of phytoplankton into or out of a locale, but also neglects the lateral processes that deliver nutrients to the subsurface. The production and advection of Subtropical Mode Water (STMW) is one such lateral process that affects the nutrient reservoir of the North Atlantic subtropical gyre.

## Nutrient depletion of the STMW during formation

STMW is formed by convection each winter in an east–west band at the northern edge of the subtropical gyre, just south of the Gulf Stream<sup>9,10</sup> (Fig. 1). As the water mass leaves the formation region, it is capped by warming surface waters in the oncoming spring, and then subducted beneath even warmer water as it travels to the south, transiting the subtropical gyre<sup>11</sup>. The nutrient concentrations in the STMW change rapidly during formation. Nutrient concentrations in the STMW formation region are consistently negligible to the base of the euphotic zone, located at roughly 120 m depth, whereas wintertime convective mixing typically reaches between 200 and 400 m depth. Thus, convective mixing entrains nutrient-rich fluid into the mixed layer, where it is combined with zero-nutrient euphotic zone water. The resulting nutrient concentrations reflect the properties of both the euphotic zone and the underlying nutricline, as well as any

ongoing biological utilization. Such utilization continuously competes with the entrainment flux of nutrients in setting the mixed layer concentrations during formation, as made apparent by the timing of the seasonal chlorophyll bloom. The initiation of the seasonal

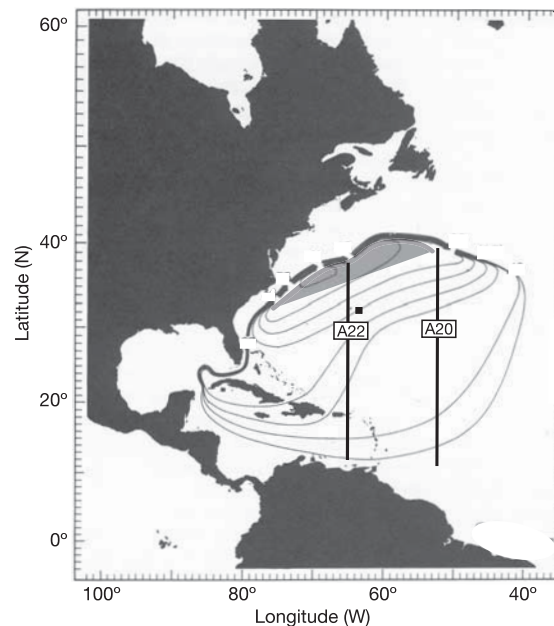


**Figure 1 | Schematic representation of the mean circulation of the warm water (>17°C) of the North Atlantic.** The filled square shows the approximate location of the BATS and Hydrostation S time series. Thick vertical lines show the WOCE repeat cruise tracks (A22 and A20) used for this study. Grey shading shows the approximate location of the STMW formation region. The solid grey lines represent streamlines with the greatest transport. Modified from ref. 11.

<sup>1</sup>Division of Earth and Ocean Science, Nicholas School of the Environment and Earth Science, Duke University, Durham, North Carolina 27708, USA. <sup>2</sup>Division of Coastal Systems Science and Policy, Nicholas School of the Environment and Earth Science, Duke University Marine Laboratory, 135 Duke Marine Lab Road, Beaufort, North Carolina 28516, USA.

chlorophyll bloom in the region of 30–40° N occurs in January<sup>12</sup>, with the maximum chlorophyll concentrations occurring in March and April. The coincidence of the winter bloom initiation with the annual solar insolation minimum precludes light as the major limiting factor in phytoplankton growth, and instead points towards nutrient limitation. The timing of the winter bloom suggests that phytoplankton are actively depleting nutrients during convective events that entrain sub-euphotic-zone water into the mixed layer. The result is that nitrate and phosphate concentrations in STMW at the time of subduction are 10–20% of those found in the upstream source waters<sup>13</sup> (see Methods), which may derive in part from eroded STMW that has joined the Gulf Stream after transiting the gyre.

### Downstream effect of STMW

The physical signature of STMW is a subsurface thermostad (a thick layer of nearly uniform temperature) centred roughly at 18 °C (Fig. 2a, c). From the representative hydrographic profiles in the subtropical gyre (Fig. 2), it is clear that the presence and thickness of the STMW varies in space and time, as does the attendant nutrient concentration below the euphotic zone. Here we use nitrate specifically for illustration, though the patterns are identical for phosphate, as the two are highly correlated for all data used in this analysis. For example, near Bermuda, downstream of the STMW formation region (Fig. 1), the mode water was roughly 400 m thick in July 1960, with nitrate concentrations below 2.5 mmol m<sup>-3</sup> to a depth of 500 m (Fig. 2a). By contrast, in July 1989 near the same site, no more than 200 m of an eroded thermostad exists, the concentration of nitrate at 500 m depth is 7.1 mmol m<sup>-3</sup>, and the integrated nitrate from the surface to 500 m is almost twice that during the same month in 1960 (Fig. 2b).

This linkage between the presence of STMW and low nutrient concentration extends to the spatial domain as well, as illustrated by two profiles taken on the same World Ocean Circulation Experiment (WOCE) survey in July 1997. The presence of STMW is clear inside the region of subtropical recirculation (Fig. 2c), but not in a more southerly profile from outside the realm where STMW resides (Fig. 2d, note the absence of a thermostad near 18 °C). The change in the nutricline depth across the subtropical gyre can be explained by the presence of the wedge of STMW, which is thickest near its source and thins southward. The underlying thermocline and nutricline move downwards to accommodate that wedge. In addition, the thermostad itself is relatively low in nutrients, so above the depressed

nutricline the inserted STMW is a low concentration ‘nutristad’. Thus, it appears that in regions and years with a strong STMW signature, low-nitrate waters reside beneath the euphotic zone. In regions and years lacking the characteristic STMW thermostad, the nutricline, no longer depressed, is a steep and nearly linear gradient between the base of the euphotic zone and the remineralized nutrients at depth.

### Spatial variability of the nutrient reservoir

The effect of the STMW on the subsurface nutrient gradient is more thoroughly demonstrated by examining a WOCE meridional section across the subtropical North Atlantic (Fig. 3). The STMW is apparent as a wedge of nearly uniform density water between the depths of 150 and 400 m, to the north of 20° N (Fig. 3a). As evidenced from an inspection of the nitrate cross-section, the presence of the STMW coincides with the deepening of the nutricline (Fig. 3b). Because mode water is convectively formed, it is characterized by a low vertical density gradient and, thus, a local minimum in the absolute value of potential vorticity (PV) (Fig. 3c)<sup>10</sup>. PV is a convenient tracer of the water mass, as it reflects the local density gradient and tends to be preserved away from the formation region as it has no internal sources or sinks. In the WOCE nutrient sections, a noticeable front in nitrate at the edge of the PV minimum (at roughly 20° N) provides evidence that STMW has a much lower nutrient concentration than surrounding water at the same density (Fig. 3d). Along a single density surface, nitrate concentrations within the STMW are roughly half that outside the zone of STMW recirculation<sup>11</sup>. These richer waters are further from their ventilation sources, and thus older.

The low-nutrient signature of the STMW, set during ventilation, can be seen more than 2,000 km to the south of the source region. This depletion persists despite the ongoing remineralization of nutrients at depth that acts to annihilate the low nitrate concentration of the water mass. The depletion also persists in the presence of vertical fluxes that act to weaken the nutristad. To understand these competing processes, the advective, remineralization and diffusive timescales have been estimated from a scale analysis of the nitrate conservation equation (see Methods). A relatively large timescale for turbulent diffusion suggests that this process is minimally important in setting the nutrient concentrations within the nutrient reservoir. However, the ratio of the advective timescale to the remineralization timescale is of the order of one within the subtropical gyre, suggesting an important competition between these two processes. Indeed, the effect of the persistent remineralization is manifested by the vertical nutrient gradient within the low-PV water mass (Fig. 3d, e). A uniform nutrient concentration within the STMW is expected at formation, yet remineralization begins re-establishing a vertical gradient once the water mass is subducted. At the PV minimum, we estimate a nitrate remineralization rate of  $0.53 \pm 0.14$  mmol m<sup>-3</sup> yr<sup>-1</sup>, too slow to completely restore STMW nitrate to its pre-formation concentration in the time it takes to transit the gyre. The relationship between STMW and nutrients implied from an inspection of the WOCE meridional sections is quantitatively assessed in Fig. 4, where PV and its corresponding nitrate concentration are plotted. Here, we are making the explicit assumption that PV is a proxy for the age of the water mass. This is an appropriate assumption given that the low-PV signature of STMW is slowly eroded over time by diffusive processes. Indeed, PV and chlorofluorocarbon (CFC) age are significantly correlated within the STMW ( $r = 0.74$ , Supplementary Fig. S1) along the WOCE sections for which CFC age is available (see Methods). Low-PV waters, indicative of recent ventilation, have lower nitrate concentrations than waters of the same density with higher PV. Using the WOCE data displayed in Fig. 4, PV is significantly correlated with nitrate ( $r = 0.86$ ).

### Temporal variability of the nutrient reservoir

Because properties of the mode water do not reflect just the response

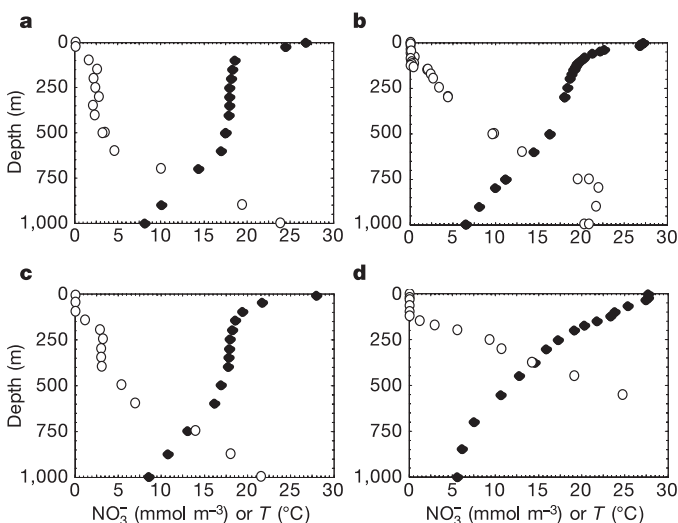


**Figure 2** | Nitrate (open symbols) and temperature (filled symbols) as a function of depth. Data are shown for: **a**, Hydrostation S (32.17° N, 64.50° W) in July 1960; **b**, BATS (31.92° N, 64.17° W) in July 1989; **c**, 30.2° N 52.3° W, from WOCE section A20 in July 1997; and **d**, 16.2° N 52.3° W, from the same WOCE section A20 in July 1997.

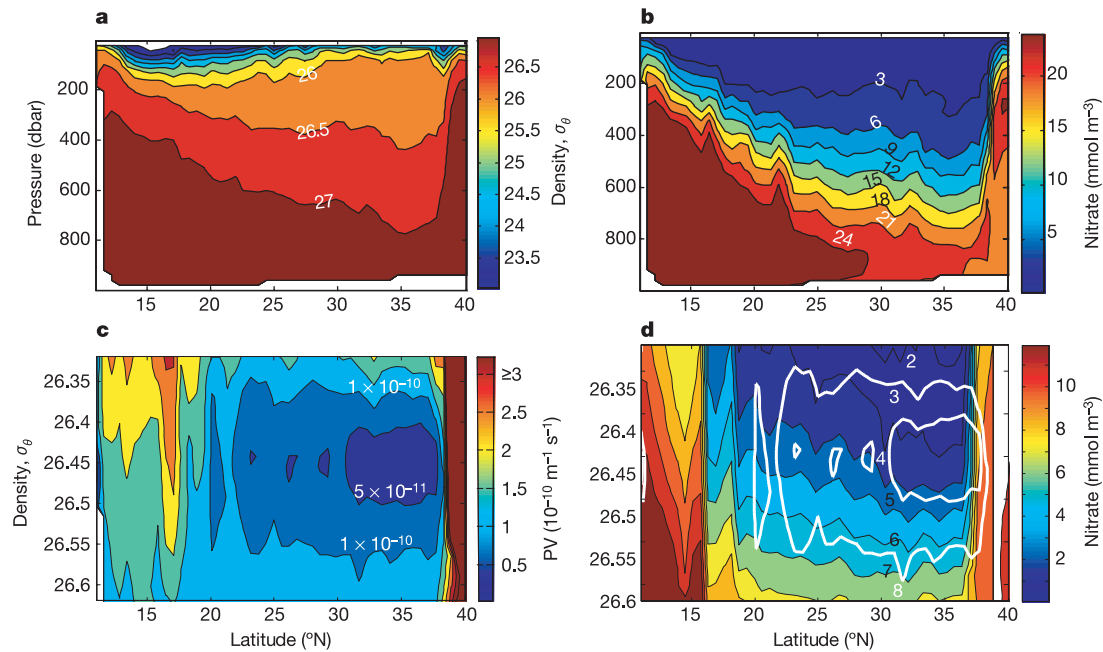


**Figure 3 | Properties of WOCE section A22 in August 1997.** **a**, Potential density as a function of pressure. **b**, Nitrate as a function of pressure. **c**, Potential vorticity (PV) as a function of potential density; the low-PV waters ( $\leq 1 \times 10^{-10} \text{ m}^{-1} \text{ s}^{-1}$ , shaded blue) are considered the core of the

STMW. **d**, Nitrate as a function of potential density. The white contour lines in **d** represent  $PV = -0.5 \times 10^{-10}$  and  $-1 \times 10^{-10} \text{ m}^{-1} \text{ s}^{-1}$ . PV was calculated using  $f/\sigma_o (\partial \sigma_\theta / \partial z)$ , where  $f$  is the Coriolis parameter,  $\sigma_o$  the reference density, and  $\partial \sigma_\theta / \partial z$  the vertical density gradient.

to the current year's forcing, but the accumulated effects of several years<sup>14,15</sup>, it is expected that extended periods of sustained deep mixing introduce interdecadal variability to the STMW nutrient reservoir downstream of the formation region. To test this expectation, two time series of nutrient data collected near Bermuda, one during the Hydrostation S programme from 1958–63 and another from the Bermuda Atlantic Time Series (BATS) programme from 1988–present, were compared. Throughout the years of the Hydrostation S observations, the North Atlantic Oscillation (NAO) was in a predominantly negative phase and relatively cold conditions in the subtropics produced dense, thick STMW. In contrast, the predominantly positive NAO regime during the BATS era caused sluggish mixing and low STMW production<sup>15,16</sup>. From our analysis, the mean nitrate concentration within the STMW is 25% higher in the positive NAO years than in the negative NAO years, a significant difference at the 1% level. Importantly, the water-column-integrated nitrate, from the surface to the top of the permanent pycnocline (nominally 400 m), is also slightly higher in the positive NAO years. This is opposite to the expectation that deeper mixing should be associated with greater nutrient availability. Instead, the time series data provide compelling evidence that low-nutrient STMW is exported to the subtropical gyre beneath the euphotic zone in periods of cold winters and intense convective mixing. As a result, the available nutrient reservoir is reduced. The correlation between PV and nitrate for the time series data (displayed in Fig. 4,  $r = 0.56$ ) indicates that the mode water present at Bermuda is most depleted in nitrate when it is most recently formed. Thus, whatever the process that moves subsurface water upwards, the delivery of nutrients will be damped in years when low-nutrient STMW occupies the subsurface nutrient reservoir.

Primary productivity from 1958–60 at Hydrostation S has been measured<sup>3</sup> using simulated *in situ* <sup>14</sup>C incubations, similar to the methods used at BATS today. Mean annual net primary productivity (NPP) from this earlier, negative NAO period was half as high as during the BATS period, 1989–2001. Wintertime maximum NPP was also slightly lower in the earlier years, never exceeding  $800 \text{ mg C m}^{-2} \text{ d}^{-1}$ , while in the BATS era, NPP exceeded that rate in 7 out of 13 years, and was double it in 1995. This is especially

surprising considering that winter mixed layer depths (MLDs) were 2–4 times deeper in the early years. Whereas the depth of winter mixing has been thought to dictate the magnitude of the winter primary productivity bloom<sup>4,5</sup>, we found no significant correlation in the BATS data between NPP and winter MLD (as chosen by a change in density from the surface of  $0.125 \text{ kg m}^{-3}$ ), regardless of averaging scheme or lag. Advective changes in the nutrient reservoir may help explain this lack of correlation. The contrast between the two periods studied at Bermuda are consistent with the hypothesis that vigorous STMW production creates a low-nutrient nutrient reservoir and exports this signal to the subtropical gyre, thereby reducing NPP downstream of the STMW formation region.

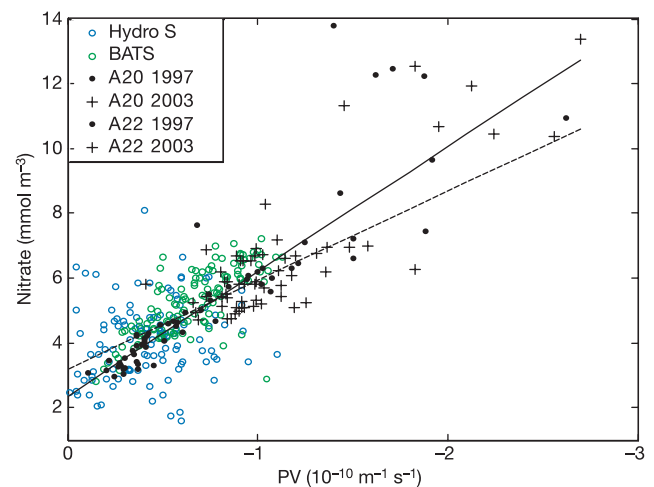


**Figure 4 | Nitrate concentration versus PV at the PV minima over the density range  $1026.45\text{--}1026.55 \text{ kg m}^{-3}$ .** Data are shown for the four repeat WOCE sections (black symbols) and the BATS (1988–2001) (green circles) and Hydrostation S (1958–1963) (blue circles) time series data. Gulf Stream data from the WOCE sections are excluded. The solid (dashed) line is the linear regression of the spatial (temporal) data.

### Competing mechanisms for nutrient delivery

Satellite observations of sea surface chlorophyll, a measure of phytoplankton standing stock, provide another means of examining the effect of STMW on the biology of the oligotrophic North Atlantic. Large-scale patterns of surface chlorophyll reveal that the subtropical gyre is not uniformly low in chlorophyll. Rather, annual mean chlorophyll constructed from climatology over the length of the SeaWiFS mission (1997–2004) is characterized by a ringed pattern, with the chlorophyll minimum located in the western limb of the central gyre (Fig. 5a). The mechanisms that determine this broad spatial pattern of surface chlorophyll remain poorly understood. To shed light on this issue, we explore qualitatively five mechanisms that possibly affect the spatial pattern of the chlorophyll fields in the subtropical North Atlantic: (1) Ekman downwelling, (2) the strength of the eddy field, (3) the depth of winter mixing, (4) supply by turbulent diffusion, and (5) nutricline displacement by the advection of STMW.

The first mechanism used to explain the location of the chlorophyll minimum is that horizontal convergence of the Ekman transport

creates downwelling such that nutrient-rich, deep water is carried further from the light field<sup>17</sup>. This hypothesis suggests that the region of maximum downwelling should approximately coincide with the chlorophyll minimum, but such coincidence is not apparent from an inspection of Fig. 5b. Furthermore, temporal changes in chlorophyll concentration and downwelling velocities contradict the idea that downwelling decreases nutrient availability: the oligotrophic region of the subtropical gyre (chosen as the fraction of the gyre with less than 0.07 mg chlorophyll  $m^{-3}$ ) shrinks at times of maximum downwelling<sup>17</sup>. In agreement with this result, we found that chlorophyll concentration and vertical velocity are negatively correlated across a broad band of the northern subtropical gyre, indicating highest chlorophyll concentrations at times of maximum downwelling. A recent study suggests that this negative correlation is explained by the lateral Ekman flux of inorganic nutrients across the subpolar/subtropical boundary during strong downwelling<sup>18</sup>. While this lateral supply may be important just to the south of the Gulf Stream, possibly reflected by the relatively high chlorophyll at the northern edge of the gyre, it is much reduced towards the centre of the gyre<sup>18</sup>.

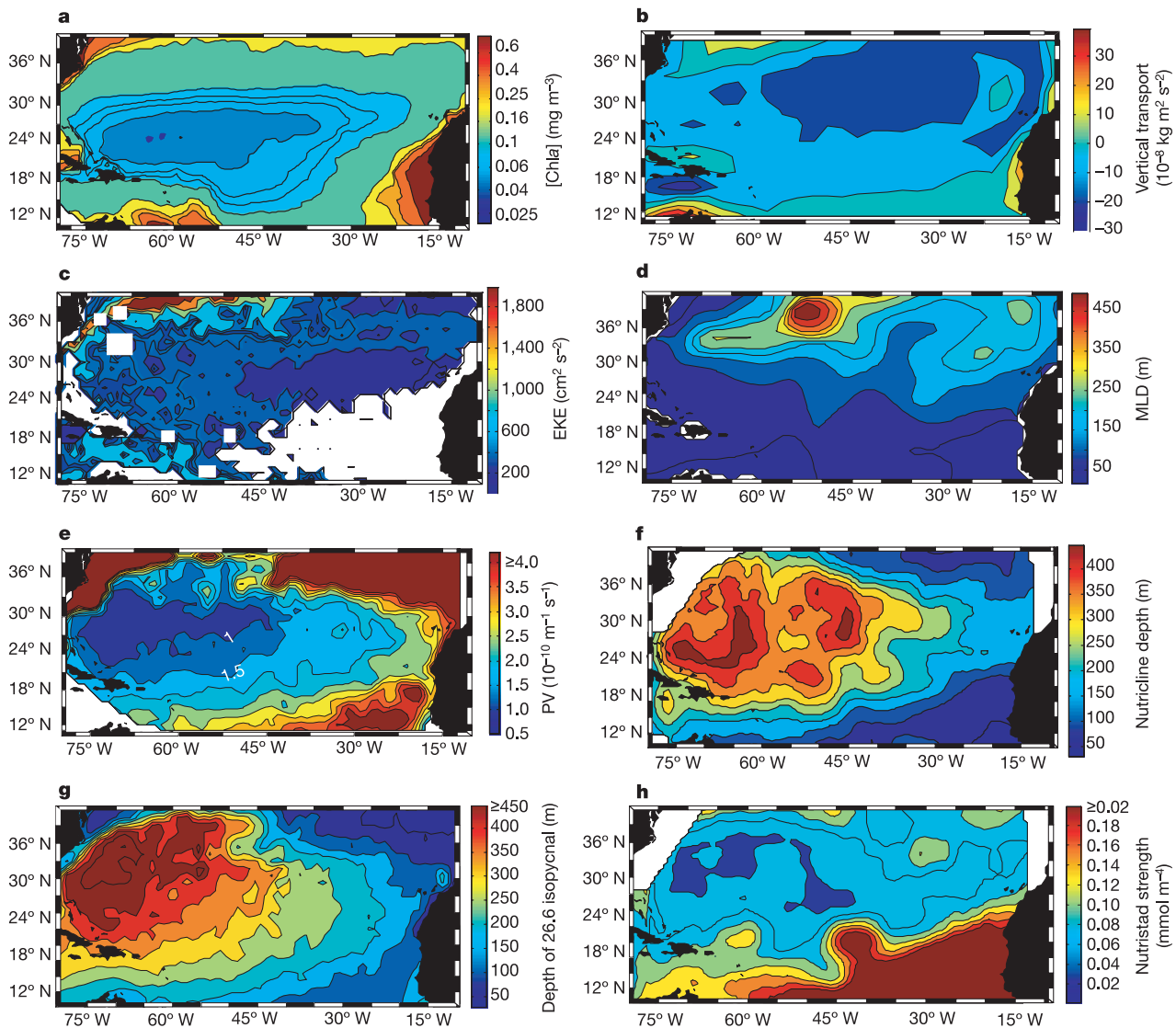


**Figure 5 | Properties of the North Atlantic subtropical gyre.** **a**, Annual mean SeaWiFS] chlorophyll *a* concentration, [Chl*a*], with a log scale for the colour axis; **b**, vertical transport calculated from the annual mean wind stress curl<sup>25</sup>; **c**, climatological mean eddy kinetic energy<sup>20</sup>, EKE; **d**, climatological March mixed layer depth<sup>26</sup>, MLD; **e**, potential vorticity on

the 26.5 isopycnal, PV; **f**, nutricline depth, as defined by the depth of the maximum vertical nitrate gradient; **g**, depth of the 26.6 isopycnal, an approximation for the base of the STMW; and **h**, the strength of the nutrient gradient at the nutricline, showing the wedge of STMW as a depleted nutrientad.

The second mechanism used to explain nutrient availability and spatial patterns of chlorophyll concentration involves mesoscale eddy events<sup>19</sup>. A passing eddy can heave a subsurface isopycnal into the euphotic zone and, if the isopycnal is high in nutrients, a surface biological response would result. Hence, it is expected that a strong eddy field, as indicated by the mean eddy kinetic energy (EKE), would correspond with a relatively high phytoplankton standing stock. The map of climatological EKE<sup>20</sup> shows a strong meridional gradient that corresponds well with the meridional gradient in satellite-measured chlorophyll (Fig. 5c). However, there is no zonal variation in the EKE field that mimics that of the surface chlorophyll field. To the contrary, EKE tends to be minimized in the eastern part of the subtropical gyre, while satellite chlorophyll is minimized to the west. Furthermore, a recent study<sup>21</sup> of the relationship between sea level anomalies, used as a measure of thermocline depth changes, and surface chlorophyll found that over much of the subtropical North Atlantic these two are not significantly correlated after the seasonal cycle was removed. The authors suggest that processes other than changes in the thermocline depth are responsible for the observed surface chlorophyll variability. To the extent that the spatial (1°) and temporal (8-day) resolution of the sea level anomaly field allows for the resolution of mesoscale eddies, this study confirms our hypothesis that eddies alone are insufficient in establishing the surface chlorophyll field.

A third mechanism that can bring nutrients to the primary producers is convective mixing<sup>4,5</sup>. It is clear from the spatial pattern of March MLD that winter mixing is deep enough to penetrate the nutricline within the STMW formation region, and perhaps slightly south of the region (Fig. 5d). Additionally, the spatial pattern of MLD resembles the surface chlorophyll map with regard to the large-scale meridional and zonal gradients (Fig. 5d). However, the closed contours of MLD do not resemble those of surface chlorophyll, and, as noted earlier, no significant temporal correlation between MLD and primary productivity exists in the time series data at Bermuda. We are left concluding that the pattern of convective mixing alone is not sufficient to establish the chlorophyll pattern within the subtropical gyre.

Turbulent diapycnal diffusion is the fourth mechanism examined here that can also supply nutrients to the euphotic zone<sup>2,22</sup>. A microstructure study conducted south of the Azores<sup>2</sup>, east of the region where STMW resides, found vertical diffusion to be an important source of nitrate to the euphotic zone<sup>2</sup>. However, a study of data from a North Atlantic WOCE section along 24°N showed that upward diffusive nitrate fluxes are much reduced in the western region of the transect where the STMW resides<sup>22</sup>. Although we lack the data necessary to examine the gyre-scale pattern of turbulent diapycnal diffusion, we infer that the nutrient characteristic of the STMW limits the vertical diffusion of nutrients, as the diffusion must act on a relatively weak gradient.

Having considered a host of vertical processes, we now examine the fifth mechanism that may act as a critical factor in setting the pattern of chlorophyll concentration: the displacement of the nutricline by STMW. The location of the STMW, as indicated by the PV minima on the  $\sigma_\theta = 26.5$  (equivalent to  $1,026.5 \text{ kg m}^{-3}$ ) isopycnal (Fig. 5e), coincides with both the region of the deepest nutricline (Fig. 5f) and the chlorophyll minimum (Fig. 5a). Because the nutricline is depressed to accommodate the wedge of STMW, its depth is roughly that of the 26.6 isopycnal (Fig. 5f, g), nominally the base of the STMW. Furthermore, because the wedge of STMW is depleted in nutrients, the strength of the nutrient gradient at the nutricline (Fig. 5h) is weakest within the STMW. The coincidence of this nutrient and the deepened nutricline with the chlorophyll minimum bolsters the hypothesis that the STMW wedge of low-nutrient water in the subtropical gyre acts to limit phytoplankton biomass. As this subsurface water mass establishes the strength of the nutrient reservoir from which all vertical processes draw, spatial patterns in biomass are best explained by a

superposition of the vertical delivery mechanisms and the nutrient reservoir.

Given the role STMW plays in establishing the subsurface nutrient reservoir in the subtropical North Atlantic, understanding the spatial and temporal variability of mode waters throughout the global ocean<sup>10</sup> could shed light on the interannual and decadal changes in global nutrient supply and primary productivity. Thus, the extent to which the mode waters are climatically variable determines the climatic variation of the subsurface nutrient reservoir and, quite possibly, that of a basin's primary productivity.

## METHODS

**Data sources.** Data used for examining STMW spatial variability are from WOCE repeat sections A20 and A22 (Fig. 1), occupied in the summers of 1997 and 2003. Time series data from Hydrostation S (32.10°N, 64.30°W) and BATS (31.92°N, 64.17°W) were both collected approximately biweekly. Hydrostation S nutrient data were collected over the period 1958–63. Primary productivity data from Hydrostation S were taken directly from Menzel and Rhyther<sup>3</sup>. Concern about whether 1960s primary productivity measurements can be compared with modern measurements is warranted, as most primary productivity work before the mid-1980s was systematically low owing to unrecognized trace metal inhibition of phytoplankton productivity<sup>23</sup>. However, a comparison of modern primary productivity measurements made with trace-metal clean methods with Menzel and Rhyther's primary productivity measurements made using a Teflon and Pyrex water sampler indicated that Menzel and Rhyther's method was free from trace metal inhibition<sup>24</sup>. Thus, we believe that the Menzel and Rhyther observations<sup>3</sup> can be directly compared with primary productivity observations from BATS.

Satellite chlorophyll data were provided by the SeaWiFS Project, NASA/Goddard Space Flight Center. They are climatological mean values, obtained at 9 km resolution over the length of the mission at the time of writing: September 1997–September 2004. The global ocean wind stress climatology used to calculate Ekman vertical velocities is based on ECMWF (European Centre for Medium-Range Weather Forecasts) analyses<sup>25</sup>. Spatial fields of EKE were calculated using float trajectories<sup>20</sup>. March MLD climatology for the North Atlantic was acquired from the Naval Research Laboratory<sup>26</sup>, with a density criterion based on a change in temperature from the surface of 0.8 °C. Basin-scale hydrographic data was acquired from the National Oceanic Data Center (NODC). Following quality control<sup>27</sup>, data from 1950–2000 were used to construct climatological PV fields at 1° horizontal resolution.

**Preformed nutrients and remineralization rate.** Nutrient concentrations in the STMW at the time of subduction were estimated by assuming that the water mass was saturated in oxygen at the time of subduction and that the apparent oxygen utilization (AOU) is caused solely by the remineralization of organic matter according to the Redfield ratio. Thus, the nitrate concentration at the time of subduction,  $N_s$ , can be estimated as:

$$N_s = N_m - \text{AOU} \times R_{(\text{NO}_3/\text{O}_2)} \quad (1)$$

where  $N_m$  is the measured nitrate concentration, AOU is the difference between the measured oxygen concentration and the saturation oxygen concentration at the observed temperature and salinity, and  $R_{(\text{NO}_3/\text{O}_2)}$  is the Redfield ratio of nitrate to oxygen<sup>28</sup>. Taking  $N_s$  at the PV minimum of each WOCE station yields an estimated nitrate (phosphate) concentration at the time of subduction of  $1.4 \pm 0.6 \text{ mmol m}^{-3}$  ( $0.05 \pm 0.04 \text{ mmol m}^{-3}$ ). For comparison, Pelegrí and Csanady<sup>13</sup> show Gulf Stream nitrate concentrations as high as  $15 \text{ mmol m}^{-3}$  for similar densities at 36°N. CFC ages have been used to calculate remineralization rates by dividing the AOU by the CFC age, and multiplying by the appropriate Redfield ratio. These CFC ages were inferred by comparing CFC-12 concentrations measured along WOCE sections A20 and A22 in 1997 to a time series of atmospheric CFC concentrations<sup>29</sup>, assuming that the surface water was in equilibrium with the atmosphere before subduction<sup>30</sup>. The correlation between CFC age and PV for both of these sections was calculated with data at the PV minima from 20–38°N, where the STMW resides.

**Scale analysis.** To compare advective, diffusive and remineralization timescales, we consider the conservation equation for nitrate:

$$\frac{\partial N}{\partial t} + \mathbf{u} \cdot \nabla N = k_H \nabla_H^2 N + k_v \frac{\partial^2 N}{\partial z^2} + R \quad (2)$$

where  $N$  is the nitrate concentration,  $\mathbf{u}$  is the velocity of a fluid parcel,  $k_H$  and  $k_v$  are the horizontal and vertical diffusivities, and  $R$  is the source of nutrients due to remineralization. The Peclet number,  $UD^2/Lk_v$ , is the ratio of the vertical diffusive timescale to the horizontal advective timescale. (Here  $D$  is the depth scale,  $L$  is the length scale, and  $U$  is the horizontal velocity scale.) This ratio is of the order of  $10^3$  using a  $k_v$  value of  $10^{-5} \text{ m}^2 \text{ s}^{-1}$ , as calculated in tracer release

experiments<sup>31</sup>; a horizontal speed of  $10 \text{ cm s}^{-1}$ ; and appropriate values of  $L$  and  $D$  for the depleted nutricline (2,000 km and 500 m, respectively). This high Peclet number reflects the dominance of horizontal advection over diffusion in setting the nitrate concentration. A similar analysis shows that along-isopycnal or horizontal diffusion is also relatively weak. The ratio of the remineralization timescale to the advective timescale,  $UN/LR$ , is calculated with the same characteristic horizontal velocity and length scale as above, a nitrate concentration ( $N$ ) of  $1 \text{ mmol m}^{-3}$ , and a remineralization rate ( $R$ ) of  $0.53\text{--}1.5 \text{ mmol m}^{-3} \text{ yr}^{-1}$ . We calculated this lower bound on the remineralization rate, as explained above. The upper bound was inferred from a previous study of oxygen utilization rates in the North Atlantic<sup>32</sup>. The resulting remineralization to advective timescale ratio ranges from 1 to 5.

Received 24 January; accepted 17 June 2005.

- Mann, K. H. & Lazier, J. R. N. *Dynamics of Marine Ecosystems* (Blackwell Science, Cambridge, Massachusetts, 1996).
- Lewis, M. R., Harrison, W. G., Oakey, N. S., Hebert, D. & Platt, T. Vertical nitrate fluxes in the oligotrophic ocean. *Science* **234**, 870–873 (1986).
- Menzel, D. W. & Ryther, J. H. Annual variations in primary productivity of the Sargasso Sea off Bermuda. *Deep-Sea Res.* **17**, 282–288 (1961).
- Gruber, N., Keeling, C. D. & Bates, N. R. Interannual variability in the North Atlantic Ocean carbon sink. *Science* **298**, 2374–2378 (2002).
- Lewis, M. R., Kuring, N. & Yentsch, C. Global patterns of ocean transparency: Implications for the new production of the open ocean. *J. Geophys. Res.* **93**, 6847–6856 (1988).
- McGillicuddy, D. J. & Robinson, A. R. Eddy-induced nutrient supply and new production in the Sargasso Sea. *Deep-Sea Res.* **144**, 1427–1450 (1997).
- Oschlies, A. & Garçon, V. Eddy-induced enhancement of primary production in a model of the North Atlantic Ocean. *Nature* **394**, 266–269 (1998).
- Sarmiento, J. L., Gruber, N., Brzezinski, M. A. & Dunne, J. P. High-latitude controls of thermocline nutrients and low latitude biological productivity. *Nature* **427**, 56–60 (2004).
- Talley, L. D. & Raymer, M. E. Eighteen Degree Water variability. *J. Mar. Res.* **40** (suppl.), 757–775 (1982).
- McCartney, M. S. The subtropical recirculation of Mode Waters. *J. Mar. Res.* **40**, 427–464 (1982).
- Worthington, L. V. *On the North Atlantic Circulation* (Johns Hopkins University Press, Baltimore, Maryland, 1976).
- Siegel, D. A., Doney, S. C. & Yoder, J. A. The North Atlantic spring phytoplankton bloom and Sverdrup's critical depth hypothesis. *Science* **296**, 730–733 (2002).
- Pelegri, J. L. & Csanady, G. T. Nutrient transport and mixing in the Gulf Stream. *J. Geophys. Res.* **96**, 2577–2583 (1991).
- Joyce, T., Deser, C. & Spall, M. A. The relation between decadal variability of subtropical mode water and the North Atlantic Oscillation. *J. Clim.* **13**, 2550–2569 (2000).
- Talley, L. D. North Atlantic circulation and variability, reviewed for the CNLS conference. *Physica D* **98**, 625–646 (1996).
- Dickson, R., Lazier, J., Meincke, J., Rhines, P. & Swift, J. Long-term coordinated changes in the convective activity of the North Atlantic. *Prog. Oceanogr.* **38**, 241–295 (1996).
- McClain, C. R., Signorini, S. R. & Christian, J. R. Subtropical gyre variability observed by ocean-colour satellites. *Deep-sea Res.* **11**, 281–301 (2004).
- Williams, R. G. & Follows, M. J. The Ekman transfer of nutrients and maintenance of new production over the North Atlantic. *Deep-Sea Res.* **145**, 461–489 (1998).
- McGillicuddy, D. J. *et al.* Influence of mesoscale eddies on new production in the Sargasso Sea. *Nature* **419**, 263–266 (1998).
- Fratantoni, D. M. North Atlantic surface circulation during the 1990's observed with satellite-tracked drifters. *J. Geophys. Res.* **106**, 22067–22093 (2001).
- Wilson, C. & Adamec, D. A global view of bio-physical coupling from SeaWiFS and TOPEX satellite data, 1997–2001. *Geophys. Res. Lett.* **29**, doi:10.1029/2001GL014063 (2002).
- Bahamón, N., Velasquez, Z. & Cruzado, A. Chlorophyll *a* and nitrogen flux in the tropical North Atlantic Ocean. *Deep-Sea Res.* **150**, 1189–1203 (2003).
- Fitzwater, S., Knauer, G. A. & Martin, J. H. Metal contamination and its effect on primary production measurements. *Limnol. Oceanogr.* **27**, 544–551 (1982).
- Barber, R. T. *et al.* Primary productivity and its regulation in the Arabian Sea during 1995. *Deep-Sea Res.* **1148**, 1127–1172 (2001).
- Trenberth, K. E., Olsen, J. G. & Large, W. G. *A Global Ocean Wind Stress Climatology Based on ECMWF Analyses* (Tech. Note NCAR/TN-338 + STR, National Center for Atmospheric Research, Boulder, Colorado, 1989).
- Kara, A. B., Rochford, P. A. & Hurlburt, H. E. Mixed layer depth variability over the global ocean. *J. Geophys. Res.* **108**, doi:10.1029/2000JC000736 (2003).
- Lozier, M. S., Owens, W. B. & Curry, R. G. The climatology of the North Atlantic. *Prog. Oceanogr.* **36**, 1–44 (1995).
- Takahashi, T., Broecker, W. S. & Langer, S. Redfield ratio based on chemical data from isopycnal surfaces. *J. Geophys. Res.* **90**, 6907–6924 (1985).
- Walker, S. J., Weiss, R. F. & Salameh, P. K. Reconstructed histories of the annual mean atmospheric mole fractions for the halocarbons CFC-11, CFC-12, CFC-113, and carbon tetrachloride. *J. Geophys. Res.* **105**, 14285–14296 (2000).
- Warner, M. J. & Weiss, R. F. Solubilities of chlorofluorocarbons 11 and 12 in water and seawater. *Deep-Sea Res.* **132**, 1485–1497 (1985).
- Ledwell, J. R., Watson, A. J. & Law, C. S. Evidence for slow mixing across the pycnocline from an open-ocean tracer-release experiment. *Nature* **364**, 701–703 (1993).
- Jenkins, W. J. Oxygen utilization rates in North Atlantic subtropical gyre and primary production in oligotrophic systems. *Nature* **300**, 246–248 (1982).

**Supplementary Information** is linked to the online version of the paper at [www.nature.com/nature](http://www.nature.com/nature).

**Acknowledgements** We thank P. Lethaby for the Hydrostation S data, D. Fratantoni for the EKE data, and D. LaBel and W. Smethie for the CFC age data. This Article also benefited from discussions with M. Follows and W. Jenkins. This work was supported by an NSF Graduate Research Fellowship.

**Author Information** Reprints and permissions information is available at [npg.nature.com/reprintsandpermissions](http://npg.nature.com/reprintsandpermissions). The authors declare no competing financial interests. Correspondence and requests for materials should be addressed to J.B.P. ([jbp3@duke.edu](mailto:jbp3@duke.edu)).